The influence of Mn on the crystallography and electrochemistry of non-stoichiometric AB5-type hydride-forming compounds

Journal of The Electrochemical Society, **146** (9) 3181-3189 (1999)
S0013-4651(98)12-048-7 CCC: $7.00 © The Electrochemical Society, Inc.

The Influence of Mn on the Crystallography and Electrochemistry of Nonstoichiometric AB_5-Type Hydride-Forming Compounds

P. H. L. Notten,[a,*] M. Latroche,[b] and A. Percheron-Guégan[b]

[a]*Philips Research Laboratories, 5656 AA Eindhoven, The Netherlands*
[b]*LCMTR, Centre National de la Recherche Scientifique, UPR 209, 94320 Thiais Cedex, France*

To design Co-free, low-pressure, hydride-forming compounds for application in rechargeable nickel metal hydride batteries, nonstoichiometric AB_x materials were investigated. The influence of both the Mn content and the degree of nonstoichiometry on the crystallography, electrochemical cycling stability, and electrode morphology were studied. The investigated composition was in the range of $La(Ni_{1-z}Mn_z)_x$ with $5.0 \leq x \leq 6.0$ and $0 \leq xz \leq 2.0$. The annealing temperature was essential in preparing homogeneous compounds. In agreement with geometric considerations, both the *a* and *c* axis of the hexagonal unit cell increase with increasing Mn content. In contrast, the *a* axis decreases with increasing degree of nonstoichiometry. As proved by neutron-diffraction experiments, the introduction of dumbbell pairs of Ni or Mn atoms on the La positions in the crystal lattice is responsible for this behavior. The electrochemical cycling stability is found to be strongly dependent on both the chemical and nonstoichiometric composition. Electrochemically stable materials are characterized by the absence of a significant particle-size reduction upon electrode cycling, reducing the overall oxidation rate. Unstable materials suffer from severe mechanical cracking through which the oxidation rate is increased. The improved mechanical stability is attributed to the reduced discrete lattice expansion. The most stable compound has a partial hydrogen pressure of only 0.1 bar, which matches well with that desirable in practical NiMH batteries. Neutron-diffraction experiments confirmed the hypothesis that La atoms are replaced by dumbbell pairs of Ni, in the case of the binary $LaNi_{5.4}$, and by Mn atoms in the case of the Mn-containing nonstoichiometric compounds. Electron-probe microanalyses and density measurements support the dumbbell hypothesis.

Manuscript submitted December 15, 1998; revised manuscript received May 28, 1999.

From a commercial point of view, the introduction of rechargeable nickel-metal hydride (NiMH) batteries has been very successful in the last decade.[1,2] This new battery type has become a serious competitor for the more conventional nickel-cadmium (NiCd) system due to its higher storage capacity and because of obvious environmental advantages. Almost all of the present-day NiMH batteries employ stoichiometric or close to stoichiometric multicomponent AB_5-type compounds as hydride-forming anode materials. These materials have proven to possess excellent electrode properties such as high storage capacity, fast activation, long cycle life, and perfect electrochemical charge/discharge rate capability. It has been argued that Co forms an essential constituent within these alloys, providing a long cycle life.[1,2] Since Co is considered to be a strategic and costly metal, however, this has an appreciable impact on the overall battery materials cost. Evidently, this cost aspect is becoming a very dominant issue, not only for the portable electronic industry but also for the future electric (hybrid) vehicle industry.

Recently, it has been discovered that cycling stability can also be significantly improved by leaving the stoichiometric AB_5 composition, *i.e.*, by making use of the as-denoted nonstoichiometric (AB_x) compounds.[3-6] Advantageously, Cu-containing overstoichiometric AB_x compounds, with $x > 5.0$, turned out to have excellent cycle life without making use of any Co. These excellent electrode properties have been related to the inhibited particle-size reduction, generally induced by the hydride formation and decomposition process through which the overall corrosion rate in alkaline electrolyte is also significantly reduced. It has been argued that the inhibited particle-size reduction was due to the introduction of dumbbell pairs of B-type atoms on the A-type positions in the hexagonal crystal lattice of the AB_x compounds.[3] As a consequence, the discrete lattice expansion was found to be significantly reduced or even absent, resulting in the good mechanical materials properties and hence, excellent cycling stability.[4] In these fundamentally oriented studies no attention was paid to more practical materials characteristics important for optimum battery operation.[3-6] For example, in the case of the reported stable Cu-containing nonstoichiometric materials, the hydrogen pressure at which the hydride formation/decomposition reaction takes place was of the order of a few bars, which is rather high for practical applications. The same strategy as outlined here was very recently also adopted by Vogt *et al.*[7] They similarly reported significant cycle-life improvements for nonstoichiometric, Sn-containing, AB_{5+x}-type compounds.

It is well known that partial hydrogen pressure can be regulated carefully by introducing other chemical elements in hydride-forming compounds. With Miedema's rule, the influence of other elements on the hydrogen pressure can be calculated simply.[8] Several metals turned out to be good candidates in lowering the plateau pressure.[9-11] Mn, nowadays widely applied in commercial stoichiometric hydride-forming compounds, is one of the most favorable metals among these. A clear relationship, on the one hand, between the unit cell volume of $La(Ni_{1-z}Mn_z)_5$ compounds and the Mn content and, on the other hand, between the plateau pressure and the Mn content, was reported.[11] Combining the various experimental results leads to a semilogarithmic relationship between the hydrogen pressure and the dimension of the hexagonal unit cell, as represented in Fig. 1. This plot shows that Mn, which ranges between 0 and 2, is indeed very effective in reducing the plateau pressure and that the crystallographic unit cell volume can be taken as a good indication for the partial hydrogen pressure.

In the present study, the impact of Ni substitution by Mn atoms in stoichiometric and nonstoichiometric AB_x compounds is investigated. The influences of both the chemical composition and the stoichiometry on the crystallography, electrochemical cycling behavior, and the electrode morphology are described. The special substitution mechanism characteristic of these nonstoichiometric compounds has been studied in more detail by neutron-diffraction measurements for both the binary $LaNi_{5.4}$ alloy and the most interesting Mn-containing compounds. Furthermore, pressure-composition isotherms have been determined by electrochemical means at room temperature and via the gas phase at higher temperatures for the most interesting compounds. In addition, the discrete lattice expansion, induced by the hydride-formation/decomposition process, has also been investigated for these materials.

Experimental

All stoichiometric ($AB_{5.0}$) and nonstoichiometric ($AB_{5.4}$ and $AB_{6.0}$) compounds were prepared from the melt as buttons by mixing the appropriate amounts of starting materials, having a purity of

* Electrochemical Society Active Member.

S0013-4651(98)12-048-7 CCC: $7.00

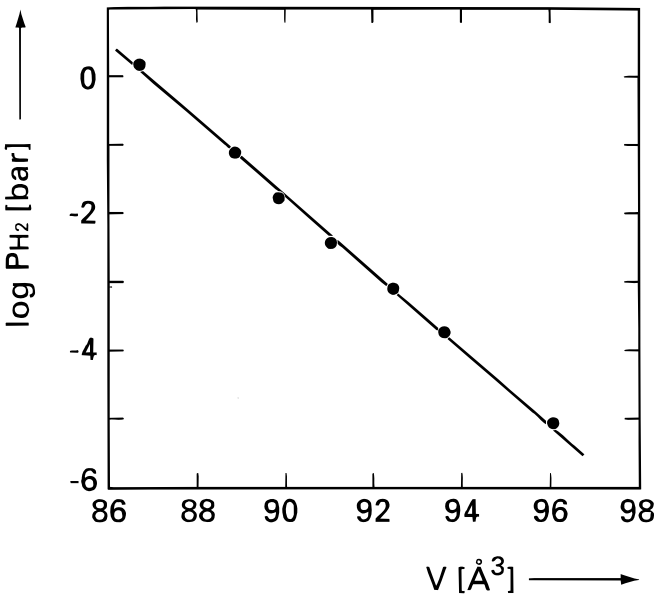

Figure 1. Logarithmic dependence of the hydrogen plateau pressure on the volumetric dimension of the hexagonal unit cell of stoichiometric $LaNi_{5-z}M_z$ compounds with varying Mn content (z) with $0 \leq z \leq 2.0$ at 25°C (from Ref. 11).

better than 99.9 wt %, and arc-melting them several times under a purified argon atmosphere to ensure homogeneity. The buttons were sealed into separate quartz tubes, containing a low argon pressure at room temperature, and subsequently annealed for 1 week at different temperatures. It has been shown that formation of single-phase compounds within the homogeneity regions is strongly temperature-dependent and is significantly influenced by both stoichiometry and chemical composition.[3-6] In order to obtain information about the homogeneity regions of the various compounds, different annealing temperatures have been applied in steps of 100°C within the temperature range 700-1200°C. As derived from conventional X-ray powder diffraction (XRD) measurements, the optimum annealing temperatures are listed in Table I. In some cases, however, small amounts of a second phase could be found, indicating that the actual composition may deviate somewhat from the nominal composition. This may also explain the measured dispersion in some of the lattice constants. As can be seen from Table I, the appropriate annealing temperature increases with an increasing deviation from stoichiometry, *i.e.*, with a larger value of *x*, and decreasing Mn content.

After cooling, the as-produced solids were mechanically ground into powders. Only the powder fractions which passed through a 50 μm sieve were used for all experiments. All powders were analyzed by XRD using conventional equipment (Philips PW 1800 powder diffractometer with Cu Kα radiation in the 10-120° 2θ range) and were in most cases found to be single-phase.

Electrodes were prepared for the electrochemical cycling experiments by mixing the sieved powders with Cu powder (Merck pro analyses) in the weight ratio of 1 to 4 and pressing these mixtures into pellets at a pressure of 4×10^8 N m^{-2}. 150 mg electrodes with a diameter of 8 mm were tested in a conventional thermostated two-compartment electrochemical cell using a 6 M KOH electrolyte, a Hg/HgO (6 M KOH) reference electrode, and a Pt counter electrode positioned in the second compartment, which was separated by a glass frit from the working electrode compartment. All experiments were performed under thermostatic control at 25°C. Galvanostatic charging was performed with a current of 350 mA/g of active hydride-forming material for 1.25 h. The electrodes were discharged with the same current until the cutoff voltage of −550 mV *vs.* Hg/HgO was reached. In order to obtain periodically the total storage capacity (C_t), the electrodes were additionally discharged every 30 cycles with a low current of 35 mA/g until the same cutoff voltage was reached. After every discharging step, the electrodes were allowed to come to equilibrium for 15 min.

Table I. Annealing temperature (°C) of the various stoichiometric and nonstoichiometric compounds prepared.

Mn content	$La(Ni_{1-z}Mn_z)_5$	$La(N_{1-z}Mn_z)_{5.4}$	$La(N_{1-z}Mn_z)_6$
0.00	800	1200	—
0.50	800	1100	—
0.75	800	1000	1100
1.00	800	1000	1100
1.25	800	1000	1000
1.50	800	900	1000
2.00	700	—	—

After the cycle experiments had been completed, the electrodes were dismantled, successively washed in water and ethanol, dried *in vacuo*, broken into two parts, embedded in an epoxy resin (Resin-5, Struers, Denmark), polished, and cross-sectionally inspected by means of optical microscopy.

Both electrochemical and gas-phase measurements were performed to determine the pressure/composition isotherms of the most interesting materials. Since the plateau pressures of the present materials are predicted to be low, the gas-phase measurements were performed at higher temperature. Prior to the isothermal measurements the samples were activated five times by exposing them to 10 bars of hydrogen gas followed by desorption under vacuum at 80°C. The isothermal desorption curves were measured at the same temperature using conventional Sievert's equipment. After the isothermal measurements were completed, the samples were partly loaded with H_2 toward *ca.* 50% of its actual storage capacity. Subsequently, the powders were removed from the Sievert's equipment and quickly transferred into an X-ray sample holder. As the equilibrium pressures for both compounds are relatively low, it is reasonable to assume that no significant desorption occurs during transfer. The X-ray spectra were measured at 20°C with a Bruker-AXS D8 diffractometer with Cu Kα radiation in the range 18-120° (2θ) by steps of 0.02°.

It has been shown that pressure-composition-temperature isotherms (PCT) can be accurately determined at room temperature by electrochemical means,[12] especially when very low pressures are involved.[13] For these measurements, the same electrochemical activation procedure was performed as described previously. After completely discharging with a low current (35 mA/g), the electrodes were intermittently charged for 30 min again with 35 mA/g under thermostatic control (25°C). During the 1 h resting period the electrode potential was allowed to come to equilibrium. The same procedure was followed during the discharging process. The partial hydrogen pressure can then be calculated from the equilibrium potential (E_{MH}^{eq}), according to[12,13]

$$E_{MH}^{eq} = -0.926 - \frac{RT}{nF} \ln\left(p_{H_2}/p_{ref}\right) \qquad [1]$$

where R is the gas constant, T is temperature, F is Faraday's constant, n is 2, the constant −0.926 is related to the hydrogen standard redox potential *vs.* the Hg/HgO reference electrode, and p_{H_2} refers to the standard pressure (p_{ref}) condition of 1 bar. This procedure was repeated 25 times for both the charging and discharging process. Discharging was interrupted at −550 mV *vs.* Hg/HgO. The electrochemical PCT measurements were performed after cycle 31, *i.e.*, after full activation and before significant degradation had taken place.

For the neutron-diffraction (ND) experiments, the two most interesting Mn-containing powders with nominal composition $LaNi_{3.75}Mn_{1.25}$ ($AB_{5.0}$) and $LaNi_{4.75}Mn_{1.25}$ ($AB_{6.0}$) were loaded into a vanadium cylindrical can. ND measurements were carried out at the Laboratoire Léon Brillouin in Saclay. The diffraction patterns were recorded on the 3T2 diffractometer at room temperature in the range of $6 < 2\theta < 125°$ by steps of 0.02° ($\lambda = 1.2272$ Å). In order to check the dumbbell hypothesis for the present nonstoichiometric

S0013-4651(98)12-048-7 CCC: $7.00 © The Electrochemical Society, Inc.

compounds, the most simple, binary compound was also investigated. This $LaNi_{5.4}$ compound was investigated at the Institute Laue Langevin in Grenoble on the D2B diffractometer between 10 and 160° in 2θ with a step scan of 0.05° and λ = 1.5966 Å. All diffraction patterns were analyzed by a whole-pattern fitting procedure, again using the program FULLPROF.[14] The Fermi lengths used (*i.e.*, the scattering factors) were b_{La} = 8.24 F, b_{Ni} = 10.3 F, and b_{Mn} = −3.73 F, respectively. The refinement procedure is described in the Results section. The neutron-diffraction samples were carefully examined by electron-probe microanalysis (EPMA). 30 data points were collected for each material, resulting in the reported average values. In addition, volumetric density measurements were performed (Accupyc 1330).

Results and Discussion

X-ray diffraction.—The XRD patterns show that all stoichiometric and nonstoichiometric compounds crystallize in the hexagonal hP6 $CaCu_5$ structure (*P*6/*mmm* space group). The lattice parameters calculated from the XRD patterns are plotted in Fig. 2 and reveal that both the *a* and *c* axis increase with increasing Mn content. As expected, substitution of Ni atoms (radius 1.246 Å) by the larger Mn atoms (dependent on the coordination number, the Mn radius is either 1.264 or 1.304 Å [15]) within the stoichiometric $AB_{5.0}$ composition leads to an increase of lattice parameters. These results are in good agreement with those found by Lartigue *et al.*[11] Considering the stoichiometric $AB_{5.0}$ structure, one A-atom position, at the 1a site, and two B-atom positions, at the 2c and 3g sites, can be distinguished in the $CaCu_5$ unit cell, as schematically indicated in Fig. 3. The partial replacement of Ni by Mn in these compounds has been investigated by neutron diffraction and has been reported to occur disorderly, but mainly in the $z = {}^1/_2$ plane at the 3g site, which is the less dense atomic plane. Only a small portion of Mn atoms was found to occupy the 2c site in the $z = 0$ plane.[11,16,17]

For the nonstoichiometric $AB_{5.4}$ and $AB_{6.0}$ compounds, similar crystallographic trends are found: both the *a* and *c* axis increase with increasing Mn content. Strikingly, the *a* axis clearly decreases with increasing deviation from the $AB_{5.0}$ stoichiometry, *i.e.*, with an increasing value of *x*. Such a dependence has also been reported for the Cu-containing nonstoichiometric materials.[3] In contrast to the Cu case, no clear dependence of the *c* axis on the degree of nonstoichiometry is found for the present Mn compounds. In order to accommodate the excess amount of B-type atoms in the nonstoichiometric materials, it has been proposed that the A-type atoms are replaced by dumbbell pairs of B-type atoms. This is also schematically represented in Fig. 3A. The dumbbell positions are denoted as the 2e sites. Consequently, due to the presence of the dumbbells, the hexagons of B-type atoms surrounding the dumbbells are induced to change their symmetry as well, resulting in the 6l sites. A planar view of the [110] plane, in which the atoms are more or less drawn to scale, makes the geometrical impact of this special substitution mechanism more clear (see Fig. 3B). Since there is much more room for the hexagons surrounding the dumbbells (Fig. 3B), it can easily be understood that the introduction of the dumbbells in nonstoichiometric compounds decreases the *a* axes of the crystal lattice (Fig. 2a). The fact that the present materials do not show a clear

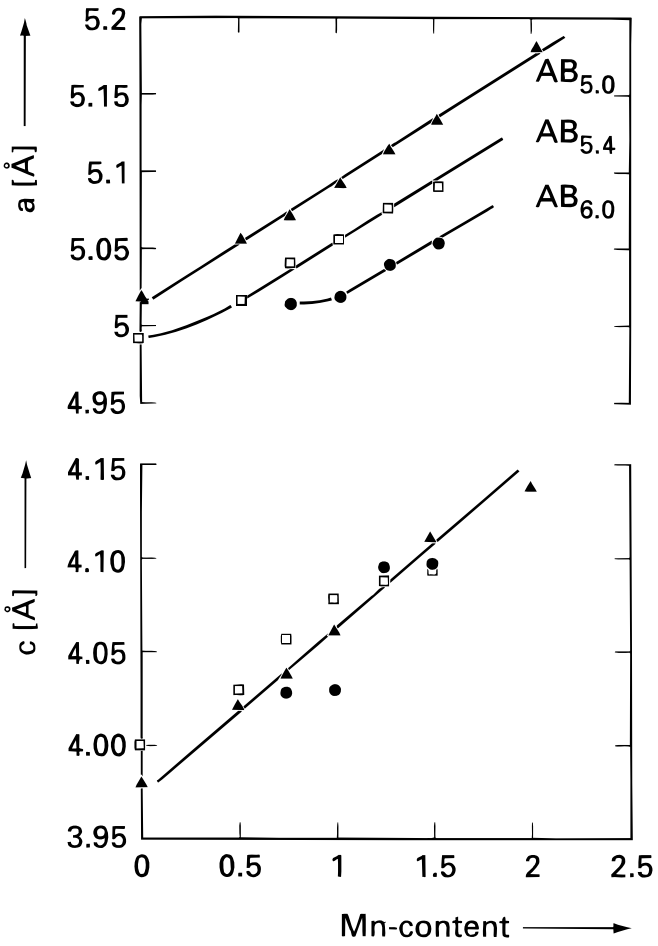

Figure 2. Dependence of the lattice constants *a* and *c* on the Mn content in (▲) stoichiometric $AB_{5.0}$ and nonstoichiometric (□) $AB_{5.4}$ and (●) $AB_{6.0}$ compounds as obtained from XRD.

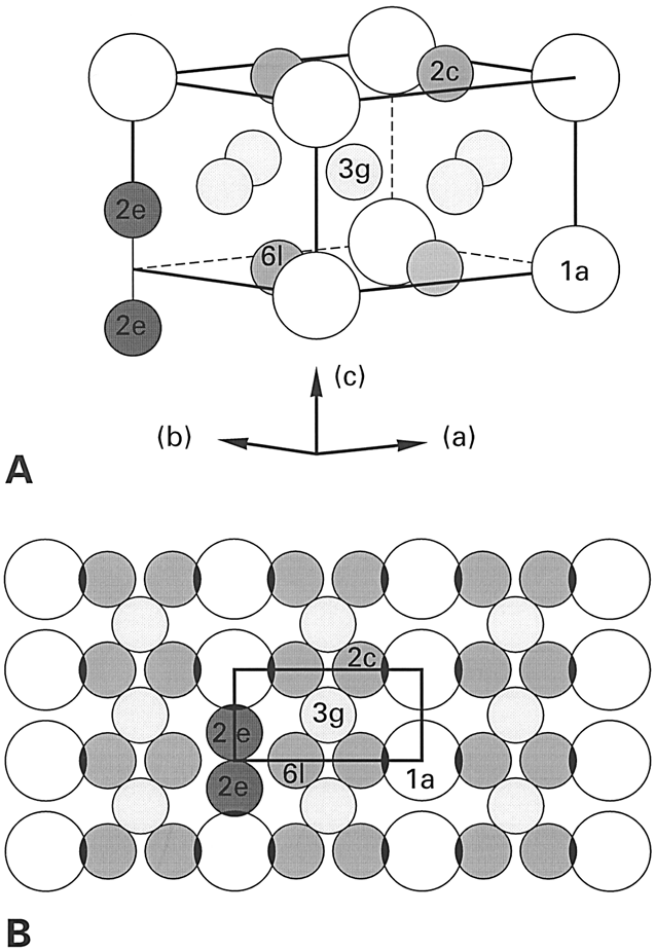

Figure 3. (A) Three-dimensional representation of a nonstoichiometric AB_x compound. The large atoms positioned at the corners of the hexagonal unit cell representing La are characterized by 1a symmetry. The smaller atoms represent the B-type atoms. The four different B-type positions to be distinguished are indicated in the two alternating z =0 and $z = {}^1/_2$ planes. (B) Planar view of the [110] plane of the same hexagonal structure.

S0013-4651(98)12-048-7 CCC: $7.00

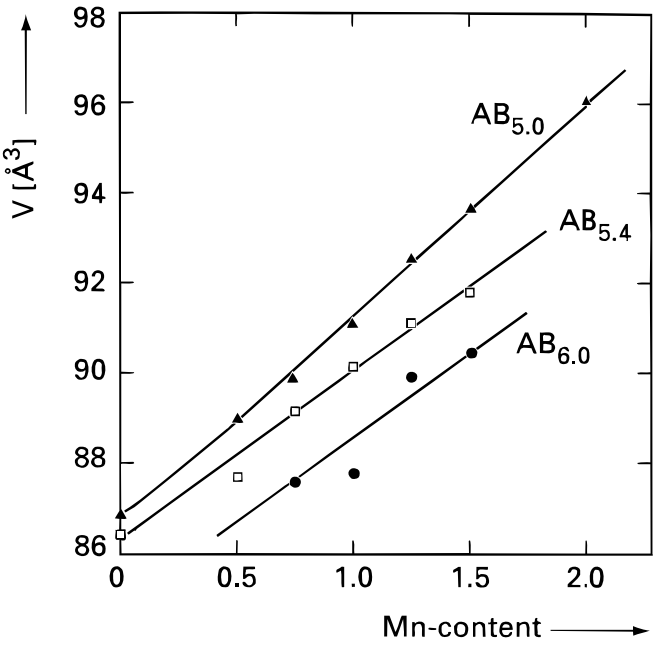

Figure 4. Dependence of calculated unit cell volume (V) on the Mn content in (▲) stoichiometric $AB_{5.0}$ and nonstoichiometric (□) $AB_{5.4}$ and (●) $AB_{6.0}$ compounds.

increase of the *c* axis, like that found in the Cu case,[3] remains to be clarified. Possibly, the inhomogeneity of some samples contributes to this equivocal dependence.

Figure 4 shows the unit cell volume (V) of the investigated compounds as a function of the Mn content, indicating that V increases with increasing Mn content and decreases with increasing the degree of nonstoichiometry. From the data shown in Fig. 1, it can indeed be inferred that the plateau pressure can be reduced several orders of magnitude by introducing Mn in to the present nonstoichiometric compounds.

The number of La replacements can be calculated as a function of the degree of nonstoichiometry by assuming that a fraction y of La atoms is replaced by $2y$ B-type atoms.[3] The general AB_x formula can be rewritten as $A_{1-y}B_{5+2y}$. Normalizing the amount of B-type atoms with respect to the A content gives the relationship between the fraction of substituted A-type atoms (y) and the overall nonstoichiometric composition (x)

$$y = \frac{x - 5}{x + 2} \qquad [2]$$

In the case of the present Mn-containing compounds in which the nominal Mn amount is denoted by z, the general formula becomes

$$La_{1-y}(Ni_{1-z}Mn_z)_{5+2y} \qquad [3]$$

Since both Ni and Mn can occupy all the four different B-type positions in the nonstoichiometric crystal lattice (see Fig. 3), each crystallographic site (i) can be characterized by the atomic ratio ζ_i, which is defined by

$$\zeta_i = \frac{Mn_i}{Mn_i + Ni_i} \qquad [4]$$

When, in addition, the number of atoms per unit cell occupying the different positions in the $CaCu_5$ unit cell is denoted by the occupancy factor τ_i, the whole system is characterized. The dependence of the total amount of Ni and Mn on τ_i and ζ_i can then be represented by

$$\sum_{i=1}^{4} \tau_i(1 - \zeta_i) = (1 - z)(5 + 2y) \qquad [5]$$

and

$$\sum_{i=1}^{4} \tau_i(\zeta_i) = z(5 + 2y) \qquad [6]$$

respectively. The various positions are summarized in Table II. Evidently, there is a direct connection between the τ_i of the various positions and the substitution level y of these nonstoichiometric compounds. This relationship is also indicated in Table II. In the case of the 3g positions, τ_2 remains, of course, fixed at 3.

Electrochemistry.—All compounds were electrochemically tested in order to investigate their electrochemical storage capacity and cycling stability. Three typical examples of cycle-life plots are shown in Fig. 5. These examples relate to compounds with nominal composition $LaNi_{x-1.25}Mn_{1.25}$ in which the stoichiometry was varied in the range $5.0 \leq x \leq 6.0$ and the Mn content was fixed at 1.25. In the initial stages, all compounds show an increase in storage capacity. During this so-called activation process, the natural oxide covering the powder particles is broken. The charge-transfer kinetics of the hydrogen reaction is consequently improved, leading to increasing capacities. The large lattice expansion occurring upon hydride-formation/decomposition and the resulting particle-size reduction is also thought to be important for producing new, highly electrocatalytic electrode surfaces.

The initial storage capacity [$C_t(0)$ [3]], as obtained from extrapolating the low-current capacities to cycle $n = 0$, are all relatively high for the three electrode materials shown in Fig. 5. The electrochemical cycling stability has been characterized by the stability factor S(400), which expresses the ratio between the remaining storage capacity after 400 charge/discharge cycles [$C_t(400)$] and [$C_t(0)$].[3] Figure 5 reveals that both the $AB_{5.0}$ and $AB_{5.4}$ compounds suffer from severe degradation. After 400 charge/discharge cycles, only approximately 25% of the initial storage capacity is left. On the other hand the $AB_{6.0}$ is found to be remarkably stable. In this case only about 25% of the initial storage capacity is lost, leading to an S(400) value of 75%.

All electrochemical results are summarized in Fig. 6 and 7. The Mn content has practically no effect on the initial storage capacity of

Table II. Description of the crystallographic sites in nonstoichiometric $La_{1-y}(Ni_{1-z}Mn_z)_{5+y}$ compounds.[a]

Site/symmetry	Atoms	Occupancy	τ_i	$\tau_i = f(y)$	ζ_i
0 1a	La	τ_0(La)	$0 \leq \tau_0 \leq 1$	$\tau_0 = 1\text{-}y$	
1 2c	Ni, Mn	$\tau_1(Ni_{1-\zeta_1}Mn_{\zeta_1})$	$0 \leq \tau_1 \leq 2$	$\tau_1 = 2\text{-}6y$	$0 \leq \zeta_1 \leq 1$
2 3g	Ni, Mn	$\tau_2(Ni_{1-\zeta_2}Mn_{\zeta_2})$	$\tau_2 = 3$	$\tau_2 = 3$	$0 \leq \zeta_2 \leq 1$
3 6l	Ni, Mn	$\tau_3(Ni_{1-\zeta_3}Mn_{\zeta_3})$	$0 \leq \tau_3 \leq 2$	$\tau_3 = 6y$	$0 \leq \zeta_3 \leq 1$
4 2e	Ni, Mn	$\tau_4(Ni_{1-\zeta_4}Mn_{\zeta_4})$	$0 \leq \tau_4 \leq 2$	$\tau_4 = 2y$	$0 \leq \zeta_4 \leq 1$

[a] τ_i is the occupancy factor of each crystallographic site and ζ_i represents the atomic ratio between Ni and Mn atoms. See text for the relations between τ_i parameters x and y. The maximum value of τ_3 is restricted to two, since y must be within the range $0 \leq y \leq 0.333$ (otherwise τ_1 would become negative, which is meaningless.

S0013-4651(98)12-048-7 CCC: $7.00

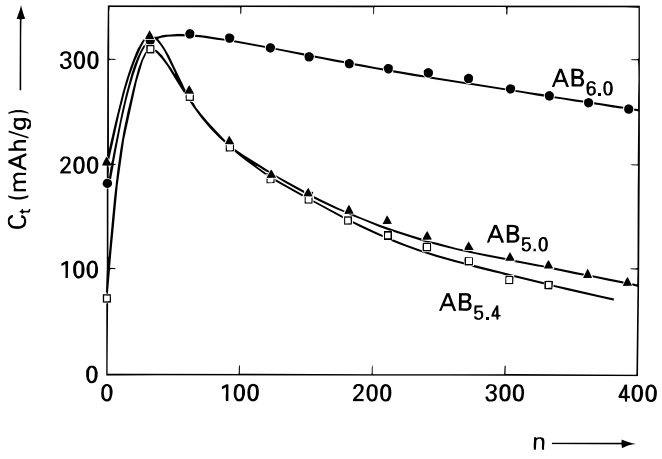

Figure 5. Cycle-life plots of stoichiometric $AB_{5.0}$ [(▲) $LaNi_{3.75}Ni_{1.25}$] and nonstoichiometric $AB_{5.4}$ [(□) $LaNi_{4.15}Mn_{1.25}$] and $AB_{6.0}$ [(●) $LaNi_{4.75}Mn_{1.25}$] compounds. Note the constant Mn content of 1.25 in all three compounds.

the nonstoichiometric compounds (Fig. 6). $C_t(0)$ decreases strongly for the stoichiometric compounds, especially at Mn contents larger than 1. This is in contradiction with corresponding gas-phase experiments where the Mn content is reported to have only little influence on the hydrogen storage capacity.[11,17] A possible explanation for this anomalous behavior could be that the plateau pressure of these materials is relatively low so that they form very stable hydrides (see Fig. 1 and 4). In order to release all hydrogen, the electrochemical driving force must be appreciable. Otherwise, not all hydrogen can be released, and the electrode will be only partly discharged.

As Fig. 7 shows, the Mn content has a positive effect on the cycling stability for the $AB_{5.0}$ compounds. It should be noted, however, that the storage capacity is relatively small for these compounds (Fig. 6). For the nonstoichiometric $AB_{5.4}$ compounds, the cycling stability is relatively poor at low Mn content, goes through a maximum, and subsequently decreases at higher Mn contents. In the case of the nonstoichiometric $AB_{6.0}$ materials, the same tendency can be seen with increasing Mn content, except that the cycling stabilities are much higher than those for the corresponding $AB_{5.4}$ compounds. In particular, the $AB_{6.0}$ compound with Mn content of 1.25

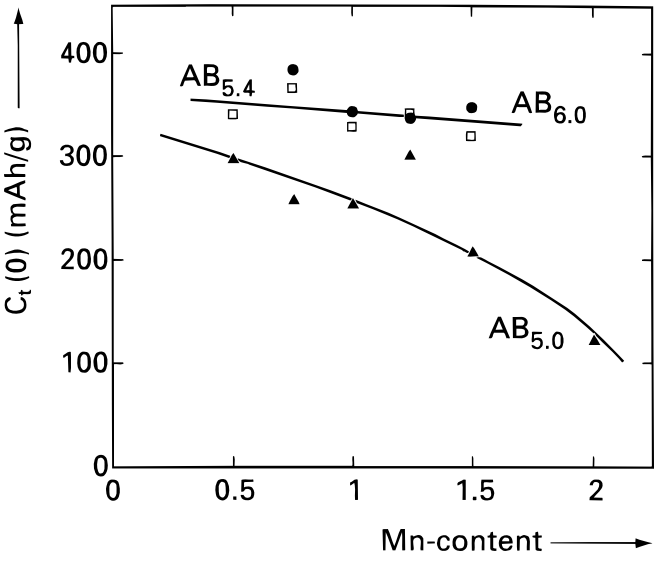

Figure 6. Extrapolated initial storage capacity [$C_t(0)$] as a function of the Mn content in (▲) stoichiometric $AB_{5.0}$ and nonstoichiometric (□) $AB_{5.4}$ and (●) $AB_{6.0}$ compounds as obtained from electrochemical cycle life experiments (see also Fig. 5).

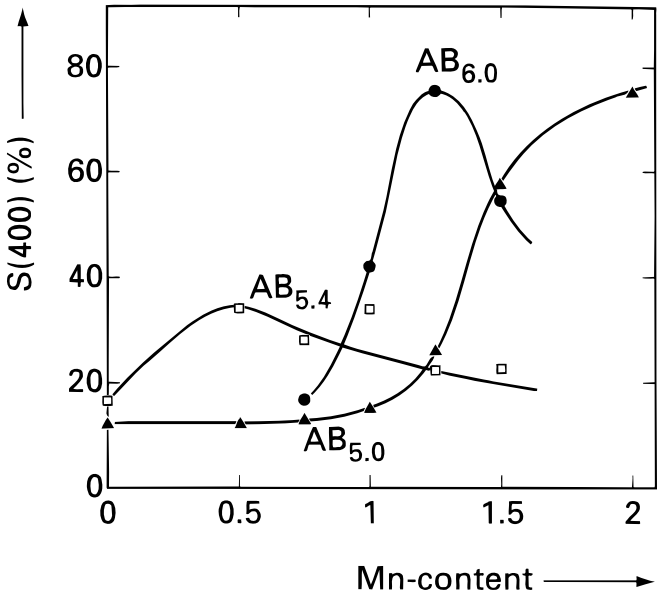

Figure 7. Calculated cycling stability factor [S(400)] as a function of the Mn content in (▲) stoichiometric $AB_{5.0}$ and nonstoichiometric (□) $AB_{5.4}$ and (●) $AB_{6.0}$ compounds as obtained from electrochemical cycle life experiments.

combines a high storage capacity with a good cycle life (see also Fig. 5). Apparently, the degree of nonstoichiometry must be considerable since the $AB_{5.4}$ compound with the same Mn content is not electrochemically stable.

Typical optical microscopy photographs of the cycled electrodes shown in Fig. 8 reveal a significant distinction in particle size for the stable and unstable compounds. Stable compounds show relative large particles even after more than 400 electrochemical charge/discharge cycles (Fig. 8b), whereas the unstable compounds consist of much smaller particles (Fig. 8a).

In order to account for the capacity loss of the various hydride-forming electrode materials upon charging and discharging in alkaline electrolyte, the following mathematical relationship has been derived

$$C_t^{1/3} = C_t(0)^{1/3} - \frac{C_t(0)^{1/3} A_o k_{ox} a_{H_2O} M_{AB_x}}{3} t \qquad [7]$$

in which C_t is the total electrochemical storage capacity at any time t in the electrode cycle life, k_{ox} is the materials oxidation rate constant, a_{H2O} is the activity of water, M_{ABx} the molecular weight of the material, and A_o is the specific surface area of the electrochemical active hydride-forming powder.[3,12] The much larger particles in the case of the stable electrodes support the concept that the cycle life is significantly improved due to the relatively small surface area (A_o) brought into contact with the electrolyte. This limits the amount of oxides formed during cycling and consequently limits, according to Eq. 7, the electrode capacity loss. A closer inspection of, for example, Fig. 8b indeed reveals the presence of approximately 1 μm thick oxide surface layers surrounding the hydride-forming powder particles formed upon prolonged cycling.

Figure 9 shows a comparison of the most informative part of the measured XRD spectra for the partly hydrided stable AB_6 compound and the unstable AB_5 hydride. Obviously, both materials reveal a clear α-to-β phase transition. The intensity of the reflections points to a 50% hydrided AB_6 compound, whereas the AB_5-hydride composition is about 60% of its maximum capacity. The lattice constants of the various phases at the plateau have been calculated from the complete XRD spectra. The calculated values are also indicated in Fig. 9. The volumetric dimension of the hexagonal unit cells can then be calculated according to

$$V_{\alpha,\beta} = \sqrt{\frac{3}{4}} a^2 c \qquad [8]$$

S0013-4651(98)12-048-7 CCC: $7.00

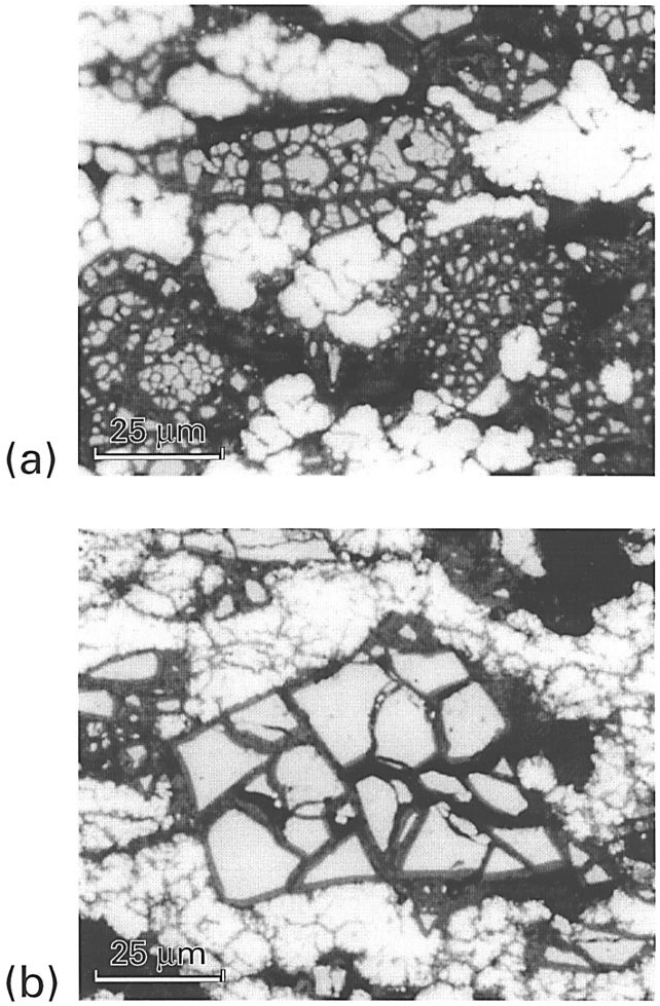

Figure 8. Typical examples of optical photomicrographs of a polished (a) stoichiometric $LaNi_{3.75}Mn_{1.25}$ electrode and (b) a nonstoichiometric $LaNi_{4.75}Mn_{1.25}$ electrode after approximately 400 complete electrochemical charging/discharging cycles.

where V_α and V_β refer to the plateau region at which, under equilibrium conditions, the α-phase corresponds to its maximum hydride content and the β-phase corresponds to its minimum hydride content. As has been defined before,[5] the volumetric lattice expansion of these phases can be related to the unit-cell dimension of the unhydrided materials (V_o) according to

$$\frac{\Delta V}{V_o} = \frac{V_\beta - V_\alpha}{V_o} \qquad [9]$$

For the present compounds, Eq. 9 reveals that the discrete lattice expansion is substantially reduced from 15.8% for stoichiometric AB_5 compound to 13.9% for the nonstoichiometric AB_6. The discrete lattice expansion was argued to be an important material property, determining the cracking behavior of the hydride-forming powders to a large extent.[5,12] The dumbbell atom pairs introduced on the 2e site (Fig. 3) were considered responsible for the decrease or even disappearance of the discrete lattice expansion and hence, for the accompanying mechanical stability. In the latter case the hydride-formation mechanism was reported to change at the as-denoted critical composition from a two-phase into a solid-solution mechanism.[5,12]

Figure 7 shows that by increasing the Mn content within the $AB_{6.0}$ series, the electrochemical stability passes through a maximum. This suggests that two processes are counterbalancing each other in this region. From Eq. 7 it seems likely that the discrete lattice expansion is suppressed with increasing Mn content and consequently, that cracking is diminished, resulting in a smaller value for A_o. The decrease in electrochemical cycling stability at higher Mn content, on the other hand, can very likely be attributed to an increased oxidation rate constant k_{ox} (Eq. 7). This indicates that the oxidation rate constant is strongly dependent on both the chemical composition of the hydride-forming compound, in this case on the Mn content (z), and the degree of nonstoichiometry (x). These results suggest that the electrochemical cycling stability can be further improved by fine-tuning both these parameters.

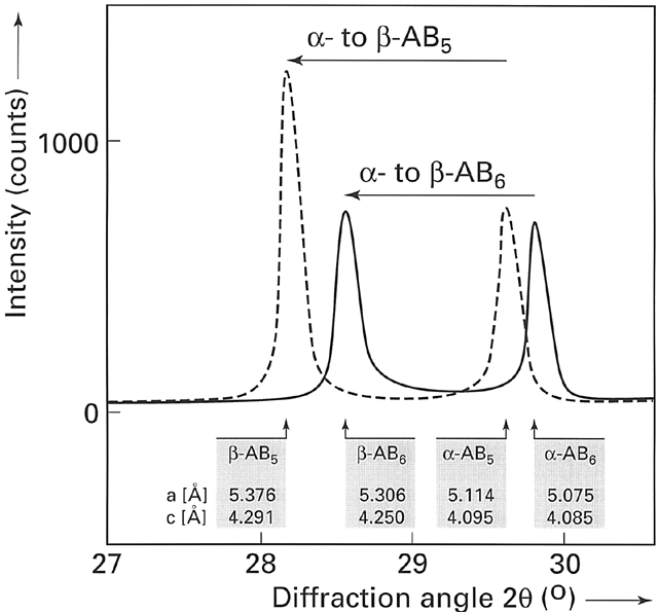

Figure 9. XRD spectra of partly hydrided (- - -) $LaNi_{3.75}Mn_{1.25}$ and (—) $LaNi_{4.75}Mn_{1.25}$ powders under equilibrium conditions at 20°C. The reflections, which can be distinguished, are indicated together with the calculated lattice constants for each crystallographic phase.

Figure 10 shows the electrochemically measured desorption isotherms at 25°C for the $AB_{5.0}$ and $AB_{6.0}$ compounds each with a Mn content of 1.25. The stoichiometric compound reveals an ex-

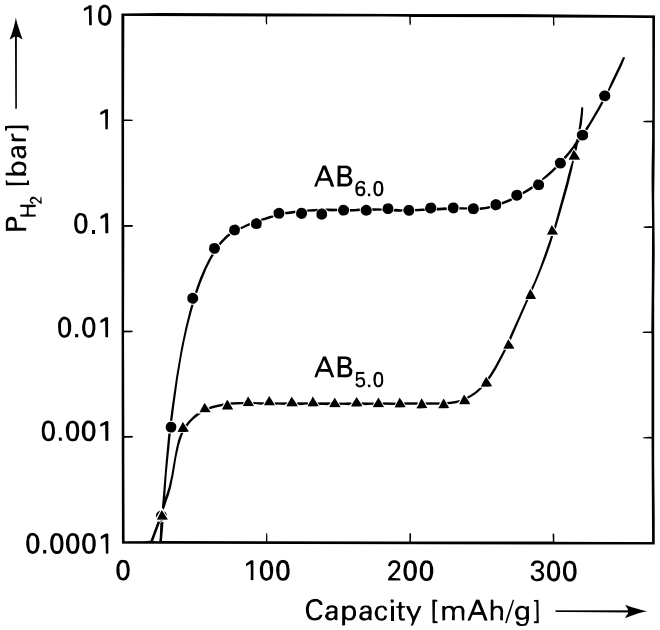

Figure 10. Desorption isotherms electrochemically determined by means of current-interruption measurements at (▲) $LaNi_{3.75}Mn_{1.25}$ and (●) $LaNi_{4.75}Mn_{1.25}$ electrodes at 25°C.

S0013-4651(98)12-048-7 CCC: $7.00

Table III. Stoichiometric and chemical composition of the three compounds subjected to ND. Calculated values correspond to the amount of each element at the preparation stage whereas the measured values are obtained from EPMA.

	$LaNi_{5.4}$		$LaNi_{3.75}Mn_{1.25}$		$LaNi_{4.75}Mn_{1.25}$	
EPMA analysis	Nominal	Measured	Nominal	Measured	Nominal	Measured
x	5.4	5.39(1)	5.00	5.13(1)	6.0	5.57(2)
y	0.054	0.053(1)	0.000	0.018(1)	0.125	0.075(1)
z	—	—	0.250	0.245(9)	0.208	0.166(1)
$La_{1-y}(Ni_{1-z}Mn_z)_{5+2y} = AB_x$	$La_{0.946}Ni_{5.108}$		$La_{0.982}(Ni_{0.755}Mn_{0.245})_{5.04}$		$La_{0.925}(Ni_{0.834}Mn_{0.166})_{5.15} + Ni_{0.55}Mn_{0.45}$	

tremely flat pressure plateau at 0.002 bar. This value is in fair agreement with what is expected on the basis of a unit-cell volume of 92.3 Å ^{3} (see Fig. 4) and Fig. 1. The plateau of the nonstoichiometric compound is almost two orders of magnitude higher and is less flat in comparison with that of the stoichiometric material. This more sloping plateau indeed points in the direction of a smaller discrete lattice expansion, which was held responsible for the increased mechanical stability of the powder electrodes.[5,12] The increase of the pressure with increasing degree of nonstoichiometry was also found with the previously reported Cu-containing materials.[4,5] However, in the present Mn case the increase is much more pronounced. Evidently, in line with thermodynamic considerations, the plateau pressures obtained via the gas phase at 80°C are higher and lie at 0.02 and 0.6 bar for $LaNi_{3.75}Mn_{1.25}$ and $LaNi_{4.75}Mn_{1.25}$, respectively. Advantageously, a plateau of 0.1 bar at room temperature and 0.6 bar at 80°C for the electrochemically stable, nonstoichiometric, compound indeed meets the currently accepted NiMH battery requirement.[2]

Neutron diffraction.—As shown in one of the previous sections, the present $La_{1-y}(Ni_{1-z}Mn_z)_{5+2y}$ system can be fully described by the parameters τ_i and ζ_i. Assuming that in each unit cell there is either a La atom or a dumbbell pair of Ni and/or Mn atoms, τ_i can be calculated from the y value for each crystallographic site, as indicated in Table II. The y values for the compounds have been determined by EPMA measurements. The B sites are assumed to be occupied by Ni atoms only, even for the Mn-containing compounds, and their occupancy factors, N_i, were refined independently. Furthermore, when Eq. 5 and 6 are taken into account, the ζ_i parameters can be obtained from the refinement of occupancy numbers N_i for each B site, where N_i is given by

$$N_i = \frac{\tau_i}{b_{Ni}}\left[(1 - \zeta_i)b_{Ni} + \zeta_i b_{Mn}\right] \qquad [10]$$

The EPMA results are summarized in Table III. the calculated nominal values correspond to the amount of each element introduced in the preparation stage, whereas the measured values are deduced from EPMA. The accuracy of the measurements is indicated between parentheses. Both data are in very good agreement for the binary compound $LaNi_{5.4}$. The stoichiometric $LaNi_{3.75}Mn_{1.25}$ compound is found to be slightly overstoichiometric, with an x value of 5.13. However, the distribution between Ni and Mn atoms is in good agreement with what is expected. Only the compound $LaNi_{4.75}Mn_{1.25}$, which is supposed to be $AB_{6.0}$, is not single-phase. The measured stoichiometry is $AB_{5.57}$, resulting in a y value of 0.075 (Table III). The excess amount of Ni and Mn is precipitated as a second phase having a composition of $Ni_{0.55}Mn_{0.45}$. From the Rietveld analyses, the amount of this second phase could be estimated to be between 5 and 6 wt %, which is in good agreement with the EPMA results.

The hypothesis of the presence of dumbbells in nonstoichiometric compounds has been tested using the simplest compound, the binary $LaNi_{5.4}$. Moreover, since all ζ_i values are zero for this compound, Eq. 10 reduces to $N_i = \tau_i$, allowing a check on the derived relationship between y and the τ_i values for the various positions listed in Table II. The crystallographic data are summarized in Table IV. Refinement of the occupancy factors leads to a y value of 0.050(2), which is in fairly good agreement with the calculated one (0.054). The various refined and calculated values for τ_i are also summarized in Table IV for comparison. The distance between the two Ni atoms forming the dumbbells can be calculated from the refined atomic z coordinate of the 2e site, according to

$$d = 2zc \qquad [11]$$

yielding a distance of 2.62(4) Å. This value is slightly larger than what is expected from the atomic radius (r_{Ni} = 1.246 Å). By using a joint refinement procedure based on both neutron and synchrotron data to be reported shortly, the calculated distance (2.49 Å) is coming very close to what is theoretically expected.[18] The presence of dumbbells is also confirmed by density measurements. These results are shown in Table V and reveal that there is very close agreement between the volumetrically determined densities and those deduced from the combined EPMA and ND experiments.

Crystallographic data for the $LaNi_{3.75}Mn_{1.25}$ and $laNi_{4.75}Mn_{1.25}$ compounds are given in Tables VI and VII, respectively. A close inspection of the ND spectrum of the latter powder indeed reveals that, in agreement with the EPMA result, a second NiMn phase is present. This phase is analyzed to have the tetragonal AuCu-type structure.

Table IV. Structural data on $LaNi_{5.4}$ with atomic coordinates (x, y, z), thermal factors (B), and refined (N_i) and calculated (τ_i) occupancy factors.

Site/symmetry	x	y	z	B	$\tau_i = N_i$ (Refined)	τ_i (Calculated)
0 1a	0	0	0	1.54(4)	0.950(3)	0.946
1 2c	1/3	2/3	0		1.698(3)	1.676
2 3g	1/2	0	1/2	1.28(2)	3.00(fixed)	3.00
3 6l	0.274(2)	2.x	0		0.302(3)	0.324
4 2e	0	0	0.327(4)		0.101(3)	0.108
Profile parameters	U = 0.103(4) V = −0.181(8) W = 0.253(4) η = 0.66(1)		Cell parameters R factors	a = 5.002(1) Å c = 4.008(1) Å R_{wp} = 4.42 R_I = 6.12	$La_{0.95}Ni_{5.10}$	r = 0.054

S0013-4651(98)12-048-7 CCC: $7.00

Table V. Density measurements.

Density (g/cm^3)	$LaNi_{5.4}$	$LaNi_{3.75}Mn_{1.25}$	$LaNi_{4.75}Mn_{1.25}$
Volumetric	8.241(4)	7.638(3)	7.836(2)
EPMA + ND	8.25(4)	7.69(6)	7.91(6)

Concerning the substitution of Ni by Mn, it is found that the dumbbells in both Mn-containing compounds almost fully consist of two Mn atoms ($\zeta_i = 100$ and 96% in Tables VI and VII, respectively). The amount of Mn on the 6ℓ site is zero for $LaNi_{3.75}Mn_{1.25}$ but reaches 25% for $LaNi_{4.75}Mn_{1.25}$. Since the amount of Mn is limited, the number of Ni atoms substituted by Mn atoms on both the 3g and 2c sites of $LaNi_{4.75}Mn_{1.25}$ is reduced. Mn preferably occupies the 3g site with respect to the 2c site in the present materials, similar to the result reported for Mn-containing stoichiometric compounds,[11] although it should be noted that the atomic ratio clearly diminishes at a higher degree of nonstoichiometry. This indicates that the introduction of a large number of dumbbells also causes the $z = 0$ plane to be less dense to some extent. The total amounts of Ni and Mn, as represented by Eq. 5 and 6 and measured independently by EPMA and ND, are compared for both compounds in Table VIII and are found to be in good agreement with each other. In addition, the density measurements performed with these compounds (Table V) are also in good agreement with those derived from the combined EPMA and ND measurements, indicating the reliability of these experimental methods.

The ND results of the present Mn-containing compounds reveal that the dumbbell positions are almost exclusively composed of Mn atoms. This strongly contrasts with the previously reported Cu-containing nonstoichiometric materials[3-5] for which it was concluded that no Cu atoms were introduced at the dumbbell position for the optimized $AB_{5.4}$ compound ($LaNi_{4.4}Cu$). In this case the dumbbells were entirely composed of Ni atoms, suggesting that the presence of dumbbell pairs in the crystal lattice rather than the chemical nature of these dumbbells is responsible for the mechanical stability of the powder particles. On the other hand, comparing the poor electrochemical cycling stability of binary $LaNi_{5.4}$ with that of $LaNi_{4.4}Cu$ clearly indicates that apart from geometrical aspects, the chemistry of the dumbbells certainly contributes to this stability.[3] This shows that the interesting role these dumbbells play in relation to the good mechanical properties is still not fully understood and needs to be investigated further.

Conclusions

The most striking aspect of the present results is that the investigated nonstoichiometric AB_x-type hydride-forming compounds can be made electrochemically stable and are characterized by low hydrogen pressures without making use of precious Co. Mn turned out to be an effective chemical element in this respect. The influence of both the amount of Mn (z) and the degree of nonstoichiometry (x) of these $La(Ni_{1-z}Mn_z)_x$ materials on the crystallography, electrochemical cycling stability, and electrode morphology has been investigated.

The optimum annealing temperature was found to be clearly dependent on the composition. The best annealing temperature to obtain homogeneous compounds generally decreases with (*i*) increasing Mn content and (*ii*) with decreasing degree of nonstoichiometry. XRD measurements confirmed that all these compounds crystallize in the hexagonal $CaCu_5$ structure. Both the *a* and *c* axis of the unit cell are found to increase with increasing amount of Mn, as expected, because Mn has a larger radius than the substituted Ni. On the other hand, by increasing the degree of nonstoichiometry, the *a* axis clearly decreases while the *c* axis remains more or less fixed.

The decrease of the *a* axis has been attributed to the fact that the excess B-type atoms are introduced into the crystal lattice by replacing part of the large La atoms by dumbbell pairs of the much smaller B-type atoms oriented along the *c* axis.[3-5] Neutron-diffraction results obtained with the binary nonstoichiometric $LaNi_{5.4}$ support

Table VI. Structural data of $LaNi_{3.75}Mn_{1.25}$.

Site/symmetry	*x*	*y*	*z*	*B*	τ_i (EPMA)	ζ_i
0 1a	0	0	0	0.89(5)	0.982	
1 2c	1/3	2/3	0		1.892	0.090(4)
2 3g	1/2	0	1/2	0.81(3)	3.000	0.34(1)
3 6l	0.29(1)	2.*x*	0		0.108	0.0(2)
4 2e	0	0	0.32(1)		0.036	1.0(3)
Profile parameters	$U = 0.345(2)$ $V = -0.345$ $W = 0.148$ $\eta = 0.38(1)$		Cell parameters *R* factors	$a = 5.107(1)$ Å $c = 4.088(1)$ Å $R_{\omega p} = 4.31\%$ $R_I = 6.49\%$		$y = 0.018$

Table VII. Structural data of $LaNi_{4.75}Mn_{1.25}$.

Site/symmetry	*x*	*y*	*z*	*B*	τ_i (EPMA)	ζ_i
0 1a	0	0	0	1.15(7)	0.925	
1 2c	1/3	2/3	0		1.550	0.070(2)
2 3g	1/2	0	1/2	0.89(3)	3.000	0.15(1)
3 6l	0.29(1)	2.*x*	0		0.450	0.25(4)
4 2e	0	0	0.32(1)		0.150	0.96(3)
Profile parameters	$U = 0.315(2)$ $V = -0.345$ $W = 0.148$ $\eta = 0.52(1)$		Cell parameters *R* factors	$a = 5.044(1)$ Å $c = 4.073(1)$ Å $R_{\omega p} = 5.47\%$ $R_I = 8.58\%$		$y = 0.075$

+ $Ni_{55}Mn_{45}$ (6 wt %)
Structure AuCu-type, s.g. *P*4/*mmm*, $a = 3.721(3)$ Å, $c = 3.538(3)$ Å, $d_C = 7.73$

S0013-4651(98)12-048-7 CCC: $7.00

Table VIII. Comparison between the Ni and Mn amounts measured by EPMA and ND analysis.

	$LaNi_{3.75}Mn_{1.25}$		$LaNi_{4.75}Mn_{1.25}$	
	EPMA	ND	EPMA	ND
Ni	3.80	3.81(7)	4.29	4.33(6)
Mn	1.23	1.23(7)	0.85	0.81(6)

this dumbbell hypothesis: the measured substitution rate is found to be in perfect agreement with that calculated. In the case of the Mn-containing compounds, ND experiments proved that the dumbbells consist of Mn atoms only. The remaining Mn atoms are distributed over the various sites in the crystal lattice. The occupation ratio of Mn atoms is found to be dependent on the degree of nonstoichiometry. The dumbbell hypothesis is also supported by EPMA and density measurements and confirms the previously reported tunneling electron microscopy results.[19] The distributions between the Ni and Mn atoms, as obtained by ND and EPMA, are also in good agreement with each other.

The electrochemical experiments reveal that the combination of the degree of nonstoichiometry and the Mn content is decisive in obtaining stable electrodes. The cycling stability was found to increase dramatically for a higher value of x. This improvement is counterbalanced by the amount of Mn introduced. In the present study an optimum was found for the nominal $LaNi_{4.75}Mn_{1.25}$ compound. Optical inspection of the electrodes after cycling revealed that the powder particles of the electrochemically stable electrodes were hardly subjected to mechanical cracking. Consequently, it can be understood that the active electrode surface area in contact with the electrolyte stays relatively small and that the electrode is less sensitive to oxidation. The unstable electrodes all suffer from a severe particle size reduction upon hydride-formation/decomposition, leading to much higher overall oxidation rates.

In line with geometrical considerations, pressure-composition isotherms revealed that Mn is very effective in reducing the plateau pressures for both stoichiometric and nonstoichiometric hydride-forming materials. The plateau pressure for the electrochemically stable $AB_{6.0}$ compound was found to be 0.1 bar at room temperature, which matches very well with what is desirable in commercial NiMH batteries. The smaller and more sloping plateau for the nonstoichiometric alloy agrees well with the smaller discrete lattice expansion, explaining the improved mechanical stability of these powders.

Fine-tuning the chemical composition and the degree of nonstoichiometry will probably lead to further improvement of the electrochemical cycling stability. In addition, it is very likely that the strategy outlined in this paper also holds for other pressure-lowering elements besides Mn and also will lead to electrochemically stable, hydride-forming materials. This would make these Co-free, nonstoichiometric compounds very attractive for application in future generations of rechargeable NiMH batteries. This holds not only for the small-size batteries now widely employed in portable electronic equipment but also, and even more importantly, for the large-scale batteries to be installed in future types of (hybrid) electric vehicles.

Acknowledgments

The authors thank H. Donkersloot and W. Gijsbers (both at the Philips Research Laboratories, Eindhoven) for preparing the intermetallic compounds and polishing the various cycled electrodes. G. Heijmans (Philips Research Laboratories) and F. Bourée-Vigneron (Laboratoire Léon Brillouinin, Saclay) are acknowledged for assisting the electrochemical and neutron-diffraction experiments, respectively.

Philips Research Laboratories assisted in meeting the publications costs of this article.

References

1. J. J. G. Willems, *Philips. J. Res. Suppl*., **39**(1), 10 (1984).
2. H. Ogawa, M. Ikoma, H. Kawano, and I. Matsumoto, in *Proceedings of the 16 International Power Sources Symposium.*, Bournmouth, T. Keily and B. W. Baxter, Editors, Vol. 12, p. 393 (1989).
3. P. H. L. Notten, R. E. F. Einerhand, and J. L. C. Daams, *J. Alloys Compd.*, **210**, 221 (1994).
4. P. H. L. Notten, J. L. C. Daams, and R. E. F. Einerhand, *J. Alloys Compd.*, **210**, 233 (1994).
5. P. H. L. Notten, R. E. F. Einerhand, and J. L. C. daams, *J. Alloys Compd*., **231**, 604 (1995).
6. M. Latroche, P. H. L. Notten, and A. Percheron-Guégan, *J. Alloys Compd*., **253-254**, 295 (1997).
7. T. Vogt, J. J. Reilly, J. R. Johnson, G. D. Adzic, and J. McBreen, *Electrochem. Solid-State Lett*., **2**, 111 (1999).
8. A. R. Miedema, *J. Less-Common Met*., **32**, 117 (1973).
9. J. Shinar, I. Facob, D. Davidov, and D. Shaltiel, in *International Symposium on Hydrides for Energy Storage*, A. F. Andresen and A. J. Macland, Editors, p. 337, Pergamon Press, Oxford (1978).
10. H. Diaz, A. Percheron-Guégan, and J. C. Achard, *Int. J. Hydrogen Energy*, **4**, 445 (1979).
11. C. Lartigue, A. Percheron-Guégan, and J. C. Achard, *J. Less-Common Met*., **75**, 23 (1980).
12. P. H. L. Notten, in *Interstitial Intermetallic Alloys*, NATO ASI Series E: Applied Science, F. Grandjean, G. J. Long, and K. H. J. Buschow, Editors, Vol. 281, p. 151, Kluwer Academic Publishers, London (1995).
13. P. H. L. Notten, M. Kremers, and R. Griessen, *J. Electrochem. Soc*., **143**, 3348 (1996).
14. J. Rodríguez-Carvajal, Abstracts of Satellite Meeting on Powder Diffraction, p. 127, Congress of International Union of Crystallography, Toulouse, France (1990).
15. E. Teatum, K. Gschneider, and J. Waber, Rep. LA-2345, U.S. Department of Commerce, Washington, DC (1960).
16. A. Percheron-Guégan, C. Lartigue, and J. C. Achard, *J. Less-Common Met*., **109**, 287 (1985).
17. A. Percheron-Guégan, C. Lartigue, and J. C. Achard, *J. Less-Common Met*., **74**, 1 (1980).
18. M. Latroche, J.-M. Joubert, A. Percheron-Guégan, and P. H. L. Notten, *J. Solid State Chem*., Submitted (1998).
19. W. Coene, P. H. L. Notten, F. Hakkens, R. E. F. Einerhand, and J. L. C. Daams, *Philos. Mag. A*, **65**, 1485 (1992).